Streaming RFID: Robust Stream Transmission over Passive RFID

Seok Joong Hwang, Youngsun Han, Seon Wook Kim, and Jong-Ok Kim

This paper proposes the streaming radio frequency identification (RFID) protocol to support robust data streaming in a passive communication, which is extended from the ISO18000-6 Type C RFID standard. By observing and modeling the unique bit error behavior through detailed analysis in this paper, we found that performance is significantly limited by inaccurate and unstable link frequencies as well as low SNR which are inevitable for passive devices. Based on the analysis, we propose a simple and efficient protocol to adaptively insert extra error control sequences in a packet for tolerating tough link condition while maximizing the throughput and preserving the minimal implementation cost. To evaluate effectiveness of our proposal in real-time streaming applications, we experimented on real-time H.264 video streaming and prototyped the system on FPGA. To our best knowledge, our paper is the first work to take analytical approach for maximizing the throughput and demonstrate the possibility of the real-time multimedia streaming transmission in the passive RFID system.

Keywords: Passive RFID, memory tag, multimedia streaming, wireless communication, protocol.

Manuscript received July 29, 2010; revised Sept. 17, 2010; accepted Oct. 11, 2010.

This work was supported in part by the System LSI division of Samsung Electronics Corporation, Ltd., and Seoul R&BD Program (10920).

Seok Joong Hwang (phone: +82 2 3290 3794, email: nzthing@korea.ac.kr), Seon Wook Kim (corresponding author, email: seon@korea.ac.kr), and Jong-Ok Kim (email: jokim@korea.ac.kr) are with the School of Electrical Engineering, Korea University, Seoul, Rep. of Korea.

Youngsun Han (email: youngsun@kiu.ac.kr) is with the School of Electrical Engineering, Kyungil University, Gyeongsan, Rep. of Korea.

doi:10.4218/etrij.11.0110.0458

I. Introduction

Passive radio frequency identification (RFID) technology has played an important role in ubiquitous computing environments. This technology enables batteryless operation and communication for a wireless device (tag). Therefore, RFID technology can enable ubiquitous deployment of wireless devices that have virtually unlimited lifetimes without incurring management costs. Widely available applications have been used by tags as an alternative to a bar-code. Adoption of passive RFID technology in applications such as inventory management and asset tracking has been extensively investigated, and thus has become mature.

Recently, several interesting approaches have emerged to adopt the batteryless feature from passive RFID technology in a variety of other compelling applications other than as an alternative to a bar-code. Those approaches break an assumption of conventional applications that a passive RFID tag can only store and provide a small piece of static data such as id codes at a low speed (640 kbps with ISO18000-6 Type C [1]). For example, sensor technologies have been incorporated with the passive RFID tag in order to obtain dynamic information about the physical world, such as temperature, acceleration, and so on [2]. There was an attempt to use a passive RFID tag for receiving audio streams without a battery in a wireless headphone [3] by extending the ISO18000-6 Type C protocol [1]. The work in [3] focused on introducing their new approach that audio streams are transferred from a reader to a tag which is attached to the wireless headphone; namely, the direction of data streaming is the opposite to other approaches. The last approach we want to particularly discuss is Memory-Spot [4] since our work focused on a similar application concept. Its goal is to transfer large amounts of rich

content from a tag to a reader at a high speed in a touching interaction range (currently, 512 kB at up to 10 Mbps with less than 5 mm) [4] by extending the preexisting protocol of low speed systems [5] with mainly extending physical parameter, that is, data transmission rates. The extremely short communication distance of Memory-Spot enables a tag to obtain sufficient power from a reader, to have a clear communication channel, and therefore, to transmit long packets, for example, tens of kilobytes, without excessive retransmission. However, when the communication distance increases, all the advantages almost disappear. The available power to a passive RFID tag is reduced, and therefore the performance of a passive RFID tag is limited in terms of timing accuracy and strength of signals transmitted by the tag as well as longer distance communication is more error-prone. In order to maximize the throughput of large data transmission at longer distance with an inexpensive solution for both reader and tag sides, we have developed an efficient error control technique through a novel packet framing method. This kind of error control is essentially required in adopting passive RFID technology in new emerging applications, particularly streaming applications which use a passive RFID tag as a streaming provider. Therefore, we believe that our work is very critical and timely, and it will be very useful for future multimedia RFID services.

In this paper, we introduce a streaming-friendly protocol extension, Streaming RFID, from a traditional and widely used passive RFID protocol, that is, ISO18000-6 Type C [1]. This extension enables robust streaming transmission from a batteryless passive RFID device while it preserves the implementation simplicity of the passive RFID system.

The major contribution in our work is to identify a unique error behavior of a passive communication system and propose a novel packet framing method that provides robust error controls for the passive RFID system. The source of the unique error behavior is an inaccurate and unstable link frequency which is a frequency of signal transmitted by a passive device (RFID tag). It makes accurate symbol synchronization difficult for a receiver. Although there have been several performance analyses for RFID systems [6], none of the works explicitly takes into account the accuracy and stability of link frequencies as well as signal-to-noise ratio (SNR) which are inevitable in the passive communication. This paper first presents a detailed error analysis, focusing on link frequencies.

The proposed Streaming RFID protocol provides adaptive insertion of two extra error control sequences, fragmented cyclic redundancy checks (CRCs), and midambles to maximize throughput under poor link conditions. Fragmented CRC was previously proposed for other wireless communication systems such as wireless sensor networks [7]. By dividing payload data into multiple fragments and inserting error-detecting codes (CRCs) for each fragment, the impact of partial packet errors can be reduced. However, it does not take into account poor synchronization performance caused by low power, which is an intrinsic feature in passive RFID. We found that the fragmented CRC alone cannot work effectively in our passive communication system. The midambles have been used in several protocols of high-end active communications for enhanced synchronization and channel estimation in time-varying channels [8]. In our proposed protocol, midambles are used to provide symbol synchronization recovering points to alleviate passive RFID's innate link frequency problem. In the field of the passive RFID technology, similar work is found in [9]. The work includes two fixed additional synchronization sequences; one is in the middle of a packet, and the other is at the end of the packet. Unlike our proposal, this fixed framing may be inefficient under dynamic link conditions. Note that the variations of link frequency may be very high and random, depending on the intensity of the available power. Thus, dynamic adaptation to the frequency variant is essential, and the interval of midamble insertion is adaptively chosen in our work. Also, we propose the mechanism of fragmented CRCs, and it is cooperatively combined with midambles for robust error control. Our proposal is the first approach with detailed analysis and evaluation in an adaptive mixture of fragmented CRCs and midambles in the field of passive communication.

By extensive evaluation, we show that the proposed Streaming RFID protocol is quite effective for real-time multimedia streaming under inaccurate and unstable link frequencies; for example, the Streaming RFID delivers H.264 video stream without loss of visual quality while conventional protocols achieve a poor visual quality (PSNR is less than 23 dB in the presence of 2.5% frequency variation in 12 dB SNR). Also, the proposed protocol does not increase implementation cost significantly. We could develop a prototype tag baseband modem at a cost of 22% hardware complexity increment from a traditional passive tag.

The paper is organized as follows. Section II presents protocol analysis which is the foundation for deriving the Streaming RFID protocol. Section III presents the Streaming RFID protocol. Section IV provides the performance evaluation of our proposal. Finally, section V concludes this research by providing implications and future research directions.

II. Protocol Design

Passive wireless communication has many restrictions on protocol design. For example, only half-duplex communication is allowed between readers and tags. Also, tags are forced to use a simple modulation scheme and support minimal

functionalities because of extremely low available power. However, packet framing is a very important protocol feature that has a great impact on communication performance. The following analysis is conducted to derive an efficient packet framing method which is practically applicable to passive communication protocols.

There are two types of packets in RFID. One is a command from a reader to tag(s), and the other is a response from a tag to a reader. In the passive RFID system, a tag transmits a response by reflecting an RF signal emitted by a reader. Consequently, the response radio signal is so weak that the wireless link is significantly error-prone. Therefore, we primarily focus on framing response packets for error-robust transmission in this paper.

Response packets in RFID are involved with additional protocol overheads, such as preambles, an error-detecting codes, and commands from a reader. It is favorable that a response packet carries as large an amount of data as possible. However, the size of a response packet is bounded because an entire packet should be retransmitted even for a single bit error. In order to alleviate this problem, we adopt a fragmented CRC scheme [7]. The method partitions a single packet into multiple fragments and adds an error-detecting code to each fragment as shown in Fig. 1(b). By the fragmentation, bit errors are localized to the corresponding fragments. Because the size of a fragment is relatively small, low fragment error rates can be achieved. Additionally, partial packet recovery is possible in a fragment basis. Thus, the retransmission overhead is considerably reduced, compared to conventional packet-based transmission, that is, packet CRC in Fig. 1(a).

However, we found that the fragmented CRC is not a strong solution in our passive communication system. The reason is that a passive tag is quite unreliable in terms of a link frequency. The link frequency is inaccurate and unstable in nature because of unstable and marginally available power to inferior oscillators. Although there have been many efforts on improving symbol timing synchronization performance with such a link frequency, it is still a difficult task due to the physical limitation of passive tags [10], [11]. Losing proper symbol timing more than one symbol period, that is, synchronization loss, results in catastrophic failure on receiving the rest of the packet. Therefore, the error localization of the fragmented CRC no longer works effectively for the rest of the packet since all remaining fragments will be corrupted from that point. The original RFID protocol allows up to ±22% of frequency error and ±2.5% of frequency variation for a tag. For simplicity, our work assumes zero average link frequency errors. This assumption is acceptable since a reader can cope with average link frequency errors by estimating the error with synchronization sequences. In addition, we expect that a reader

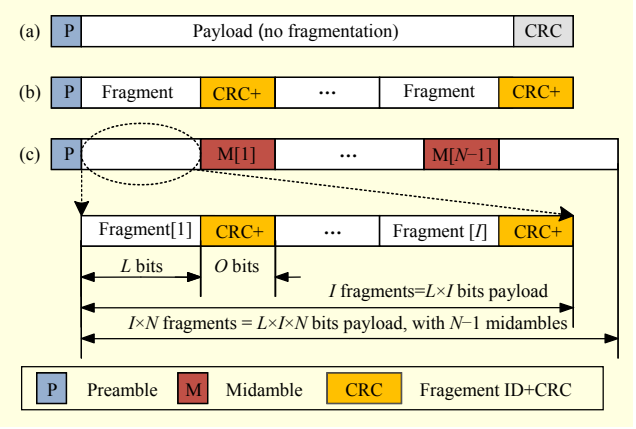

Fig. 1. Response message formats: (a) Packet CRC, (b) Fragmented CRC, and (c) Proposed format.

can take advantage of a long interaction with a single tag in our proposed system. The link frequency error highly depends on the tag's sampling resolution, thus a large amount of the error is static for a given tag. Therefore, a reader can minimize the average link frequency error by calibration based on previously monitored errors. While we ignored the large amount of frequency errors, we focused on the frequency variation problem. Therefore, it is crucially important to justify that such large variation, ±2.5%, is a practically encountered problem in real systems. A transistor level simulation reported that the worst case link frequency variation is 1.19% [12]. This is an apparently large variation range compared to ppm unit ranges of typical active communications. Also, the work in [12] used an ideal power supply model. Thus, the frequency variation ranges in practical systems may be larger than ±1.19%. However, our study examined not only the maximum variation range ±2.5% but also various variation ranges of 0%, ±0.5%, and ±1.25% at the same time.

In the following subsections, we show motivational experimental results and propose our new framing scheme which provides robust error controls for both partial bit errors and synchronization losses.

1. Error Behavior

We first analyze error behavior in response packets from a tag to a reader. This analysis uses the same simulation environment as section IV.

Figure 2 shows error probabilities of individual bits in a packet where the link frequency has neither error nor variation. This graph exhibits an important error behavior that bit error probability is dependent on the corresponding bit location in a packet. The curves monotonically increase in proportion to a distance from a preamble because symbol decoding timing offset is accumulated and hard to cancel when a bit is far from

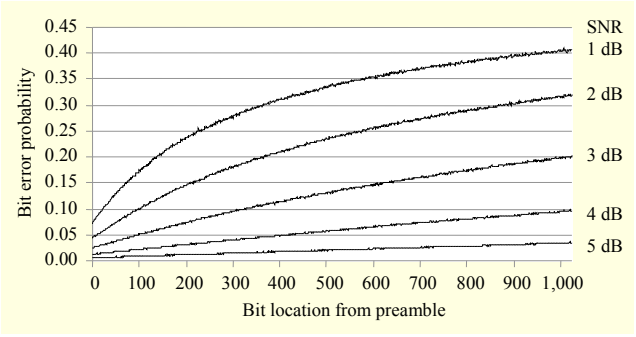

Fig. 2. Error probabilities of individual bits in a packet.

a synchronization sequence–a preamble. However, despite the exact link frequency condition, the curve slope is not flat. It is because noise affects performance of symbol decoding as well as its timing adjustment. This effect is more severe in a system where the link frequency is allowed to have a wider variation range.

For a detailed analysis, the bit error probability is modeled using data obtained from simulations, and its model is given by

$$BER(D) = 1 - \alpha \cdot \beta^{D}, \tag{1}$$

where D is the distance (measured in bits) from a preamble. Actually, the curves in Fig. 2 need a more complex model to fit all the data points exactly (we performed nonlinear least squares fitting in order to estimate model parameters). However, by restricting data points fitted to a certain range, (1) is able to model the error probability curves quite accurately. To reasonably select data points to be fit, D is restricted to satisfy the following condition:

$$PER(D) = 1 - \prod_{i=1}^{D} (1 - BER(i)) \le 0.999, \tag{2}$$

where $PER(D)$ is an error probability of a packet whose length is D, excluding a preamble. Equation (2) restricts the fitting to include the data points which make packet error probability less than 99.9%. It can be assumed that a packet containing more than D bits is always corrupted. Thus, it is not meaningful to include more data points in the fitting.

Figure 3 plots model parameters, α and β in (1), obtained from the curve fitting with several link frequency conditions of the uplink (form a tag to a reader). The link frequencies are modeled by

$$LF_{\text{tag}}(t) = LF_{\text{tag\_exact}} \cdot (1 + v \cdot \cos(2\pi f t)), \tag{3}$$

where $LF_{\text{tag\_exact}}$ is an exact link frequency (the maximum link frequency 5,120 kHz was used), v is the maximum link frequency variation, and f is the variation frequency. It models inaccuracy and instability of the link frequency. We modeled the link frequency variation simply as a sine function having

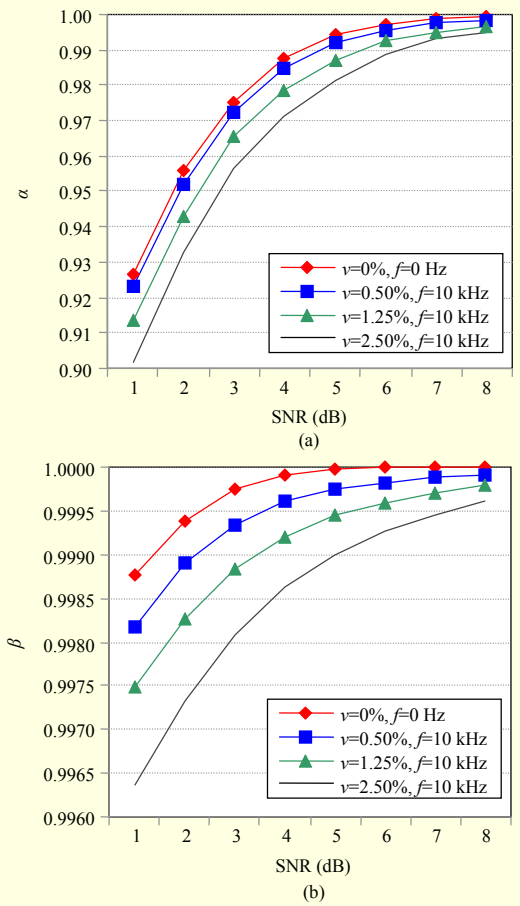

Fig. 3. Model parameters of error probability curves.

0 Hz and 10 kHz frequencies. It assumes that the link frequency smoothly and slowly varies. It will be worth using more complex models like the transistor level model [12] to exactly capture the impact of the link frequency variation. However, our model does not lead to misevaluate our findings. It is because the usefulness of our proposal is more highlighted in poor link frequency conditions. In (1), α can be interpreted as a probability of successful bit decoding when a bit is decoded within an adequate time window as intuitively illustrated in Fig. 4. The model parameter β can be regarded as a probability that decoding timing offset stays in the adequate window. Therefore, β^{D} is a probability of no synchronization loss at D-th bit. Figure 3 supports our interpretation. β decreases considerably at an inaccurate and unstable link frequency as well as low SNR, while α is fairly insensitive to link frequency conditions but sensitive to SNR.

The bit error probability model in (1) implies that, in the fragmented CRC scheme [7], decoding of the fragment to be located later cannot be effectively isolated from previously located fragments particularly with smaller β, that is, higher probability of synchronization loss. In passive communication

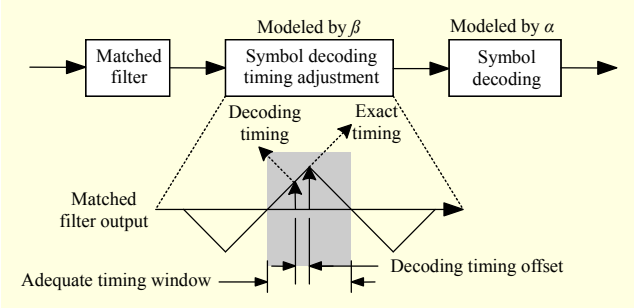

Fig. 4. Receiver model for interpretation of error behavior.

systems, β is intrinsically small due to the inaccurate and unstable link frequencies. Therefore, a primary requirement in those communication systems is to effectively control synchronization loss.

2. Proposed Method

To cope with the synchronization loss problem which was revealed in the previous subsection, we propose to insert midambles between fragments in addition to the fragmented CRCs as shown in Fig. 1(c). The midamble acts a resynchronization point in order to break dependence on the previously located fragments.

In order to evaluate the effectiveness of the midamble insertion, we first derive the effective throughput of the uplink in RFID as

$$TP = \frac{L \cdot I \cdot N \cdot (1 - \rho(R_{\max} + 1))}{T_{\mathrm{ACK}} + T_{\mathrm{RESP}} + T_{\mathrm{RETRY}}}. \quad (4)$$

The value of TP is determined by three major parameters: L is a length of each fragment in bit unit, I is a midamble insertion interval whose unit is a fragment, and N is a total number of synchronization sequences including one preamble and midambles. In TP, the numerator is an expected amount of delivered data where the number of retrials is limited to $R_{\max}$ (in reliable communication mode, $R_{\max}$ should, in theory, be ∞). The denominator in TP is a time expected to elapse before an entire packet is received successfully.

T_{RESP} indicates the transmission time of a response message, and it is expressed by

$$T_{\mathrm{RESP}} = \frac{S_{\mathrm{pream}} + S_{\mathrm{mid}} \cdot (N-1) + (L+O) \cdot I \cdot N}{LF_{\mathrm{tag}}}, \quad (5)$$

where S_{pream} and S_{mid} are the number of bits in a preamble and a midamble, respectively, and O is per-fragment overhead.[1)]

T_{RETRY} represents time to be consumed for retransmissions, and it is given by

$$T_{\mathrm{RETRY}} = \sum_{r=1}^{R_{\max}} T_{\mathrm{NACK}} \cdot \psi(r) + T_{\mathrm{RESP}} \cdot \rho(r). \quad (6)$$

T_{ACK} in (4) and T_{NACK} in (6) represent the time required for transmitting ACK and NACK commands, respectively. Since T_{NACK} contains mask bits of fragment errors in the previous trial, it is longer than an ACK command transmission time (T_{ACK}). T_{NACK} is obtained by[2)]

$$T_{\mathrm{NACK}} = T_{\mathrm{ACK}} + \frac{I \cdot N}{LF_{\mathrm{reader}}}, \quad (7)$$

where $\rho(r)$ in (4) and (6) is a probability of failure to receive a fragment during r trials. $\psi(r)$ in (6) is a probability of failure to receive a complete packet during r trials. Those are given by

$$\rho(r) = \left(\sum_{i=1}^{I} FER(L+O,\ i) / I\right)^r, \quad (8)$$

$$\psi(r) = 1 - \left(\prod_{i=1}^{I} 1 - FER(L+O,\ i)\right)^{I \cdot N \cdot \rho(r-1)}, \quad (9)$$

where $FER(l, i)$ is the error probability of the i-th ($1 \le i \le I$) fragment whose length is l, and it is given by

$$FER(l,i) = 1 - \prod_{k=l(i-1)+1}^{l \cdot i} \alpha\beta^k = 1 - \alpha^l \beta^{(2l^2 i - l^2 + l)/2}. \quad (10)$$

Finally, we find out optimal packet framing parameters (L^*, I^*, N^*) to maximize the effective throughput, TP in (4). For given link condition parameters (α and β which determine performance of symbol decoding and synchronization, respectively), the optimal packet framing parameters are obtained by

$$\{L^*, I^*, N^*\} = \max_{L,I,N} TP. \quad (11)$$

Even though the fragmented CRC and the midamble insertion were already introduced [7], [8], our work is the first approach to overcome both partial bit errors and synchronization losses in the passive communication by combining the two techniques.

III. Streaming RFID Protocol

This section describes how to extend the ISO18000-6 Type C protocol for video streaming and how to use the extended streaming RFID protocol. At first, we redefined the physical parameters of the protocol. The original protocol supports up to a 128 kHz downlink (from a reader to tag(s)) and a 640 kHz

1) In this work, the same 18-bit synchronization sequence is applied for both preamble and midamble. O is 20: 4-bit fragment ID and 16-bit CRC. O is just 16 if fragmentation scheme is not applied.

2) T_{ACK} is around 37.74 μs including the packet itself (with a 32-bit command code) and required time intervals from a response to a command and vice versa. LF_{reader} and LF_{tag} are link frequencies of the downlink and the uplink: 1,024 kHz and 5,120 kHz, respectively.

uplink (from a tag to a reader) frequencies. For rapid data transmission, we increased the frequencies eight times like Memory-Spot: 1,024 kHz and 5,120 kHz, respectively, to enable streaming transmission of H.264 videos in baseline profile level 2.x (2 or 4 Mbps).

Several preexisting commands to be used for accessing small amounts of data were replaced with new send back (SB*)* commands (*SB-CONT*, *SB-ACK*, *SB-NACK*, and *SB-JUMP*) to realize streaming transmission control as well as the proposed packet framing method (adaptive embedding of midambles along with fragmented CRCs). In addition, one protocol state (*Data*) was added for the new commands. The original *Kill* command was removed because, unlike in logistic applications, there was no need for permanent device destruction. It fully supports a preexisting inventory (identification) feature among multiple tags. A security feature is also preserved because the *Data* state for the new commands can be reached through a preexisting *Secured* state if it is protected by a password. The new commands can be executed only with a proper dynamic handle for avoiding disorder in multiple tag and reader environment. The roles of the new commands are the following:

- *SB-CONT* initiates streaming transmission. Also, it can be used for non-sequential memory access. It contains i) 10 bit command, ii) 16 bit dynamic handle obtained from a target memory tag, iii) 32 bit address to support 4 GB memory space, iv) 9 bit response packet framing parameters (*L*, *I*, *N*) encoded in each 3 bits to indicate $\log_2$ of those values (for *L*, byte unit is used), and v) 16 bit CRC–83 bits in total. A target tag transmits a response with data addressed by this command in the format of Fig. 1(c).
- *SB-ACK* continues streaming transmission. It consists of i) 10 bit command, ii) 16 bit dynamic handle, and iii) 5 bit CRC–31 bits in total. A target tag transmits a response with succeeding data of the last transferred one.
- *SB-NACK* is to recover broken fragments in the last transferred response. It has the similar format with SB-ACK, but it includes a retransmission mask whose size is equal to the fragment count, so that a target tag transfers only broken fragments for partial packet recovery.
- *SB-JUMP* is to skip several data to be transmitted and to continue streaming transmission. It consists of i) 10 bit command, ii) 16 bit dynamic handle, iii) 12 bit jump offset, and iv) 5 bit CRC–43 bits in total. A target tag transmits a response with data which is located at the jump offset plus the start point of the last transferred one. Real-time video streaming applications may exploit this command to reduce the number of useless retransmissions when current throughput is too small to meet the deadline of video data.

```
Clear MASK
For each received fragment i,
   If the fragment i was corrupted,
         MASK[i] = true
         FERC[i mod I]++
   End
   FRXC[i mod I]++
End
If all fragments are correctly received,
   ADDR += PS.
   If sum(FERC) is greater than a threshold,
         BER[0:I–1] = estimate BER from FERC/FRXC with L
         SLOPE = estimate slope of BER with I
         [L, I, N] = ADAPT_TABLE[BER[0], SLOPE]
         Clear FERC, FRXC
         Send SB_CONT(ADDR, L, I, N, TDH)
   Else send SB_ACK(TDH)
   End
Else send SB_NACK(TDH, MASK)
End
```

FERC: frag. error counters
FRXC: received frag. counters
PS : packet data size
TDH: tag dynamic handle

Fig. 5. Example of pseudo-code for adapting parameters.

With this Streaming RFID protocol, it is important to maximize throughput by adapting the three parameters (*L*, *I*, *N*). The adaptation entails monitoring the current link condition. The link condition model parameters, α and β of (1), can be derived by tracking error behavior between midambles additionally with the assistance of a symbol timing synchronizer. According to the derived values, the response parameters can be suitably adapted with a preobtained adaptation table or other closed-loop control methods for time-varying link conditions.

Figure 5 shows a pseudo-code example for adapting the three parameters in a stream data receiving loop after the reader receives fragments of a response.

In the example, the reader marks corrupted fragments on a retransmission mask (*MASK*) to be used by *SB-NACK* for partial packet recovery, and increases the corresponding fragment error counter (*FERC*) entry. The entry index is equal to the number of fragments between the previous synchronization sequence (preamble or midamble) and the corrupted fragment (*i* mod *I*). Therefore, *FERC* aggregates fragment errors which are equally affected by β since the synchronization loss probability of a fragment is determined by the distance from the previous synchronization sequence. Whenever the errors have been sufficiently collected (more than a threshold), the reader adapts the three parameters (*L*, *I*, *N*) according to the average of fragment errors (divide *FERC* by *FRXC*). BER of each average fragment error can be estimated with fragment size (*L*) using a conversion table or in a mathematical way, like $1–(1–AverageFragmentError)^{1/L}$. Estimating β requires huge tables or complex calculations such as nonlinear regression. For implementation simplicity, this example uses an estimated slope (*SLOPE*) of the BERs instead of actual β because the slope is determined or obtained by simple linear regression methods. Therefore, the parameter adaptation is based on the offset (*BER*[0]) and slope (*SLOPE*) of the estimated BERs. Also, *ADAPT_TABLE* is employed to

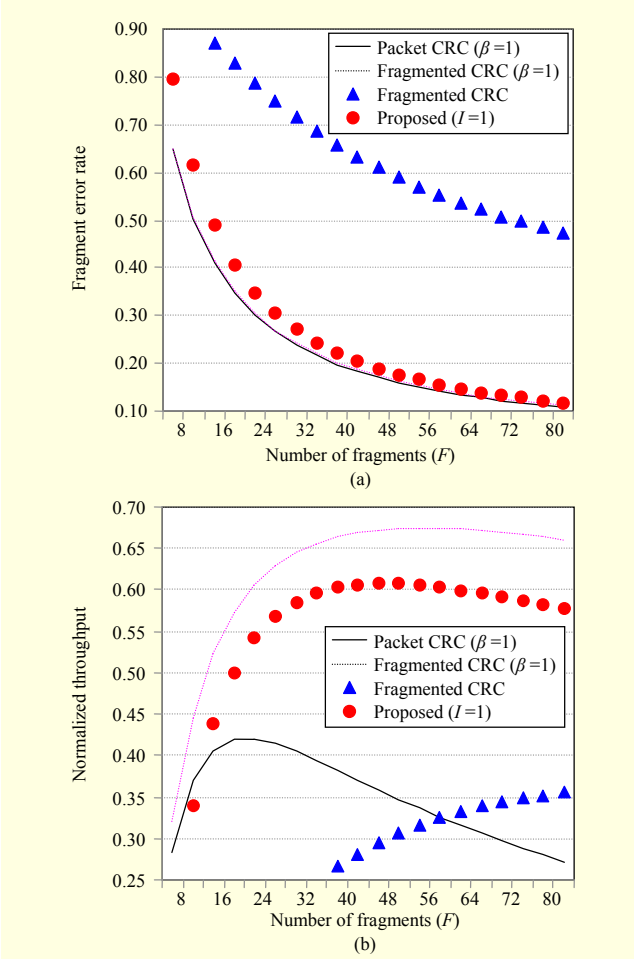

Fig. 6. Fragment error and throughput of each framing scheme at α=1–10^{-3}, β=1 and 1–10^{-6}.

obtain the best suitable parameters (L, I, N). The table can be predefined through experiments.

IV. Evaluation

This section evaluates the Streaming RFID protocol. We first demonstrate the effectiveness of the proposed protocol in terms of data throughput. Then, as a promising application, we apply the proposed protocol to real-time video streaming. In addition, we evaluate the impact of the Streaming RFID protocol on the hardware implementation with making a prototype of a tag.

For evaluations, we used the Monte Carlo simulation with a reader's receiver model [10] and additive white Gaussian noise channel. Briefly, the receiver model used a bank of 12 correlators for preamble detection to cover a wide range of link frequency errors. For calibrating symbol decoding timing, the Early-Late gate algorithm was used, and the oversampling rate was 4. The simulations for bit error probability, shown in Fig. 2, were repeated 100,000 times for each parameter. The rest of evaluations were based on the bit error probability results in order to reduce simulation time.

1. Determining Packet Framing Parameters

At first, we evaluated our proposed packet framing scheme for several link model parameters: α and β in (1). Figure 6 plots fragment error rate and normalized throughput for each scheme when the number of fragments (F) is varying.[3)]

Packet CRC (conventional scheme) has only one fragment (I=1, N=1, L=128 B×F^{-1}): in this case, F is used only for varying packet length, not for the actual fragment count. Figure 6(a) shows that the fragment error rate ramps up dramatically as F decreases, that is, the fragment/packet length L increases. Although it is possible to maximize throughput by choosing the best fragment size according to link condition, the achievable throughput is quite limited: just about 42.1% of the ideal throughput at α=1–10^{-3} and β =1 as shown in Fig. 6(b).

In the same link condition, prominent throughput improvement is achieved by the fragmented CRC (I=F, N=1, L=128 B×F^{-1}). At condition of high β value, that is, accurate and stable link frequency, the fragmented CRC performs effectively. However, when β is configured with 1–10^{-6}, its effectiveness drastically reduces; the normalized throughput is reduced from 67.5% to 36.3%. It is because the fragment error rate cannot be effectively suppressed solely by fragmentation (Fig. 6(a)).

To cope with this problem, we insert midambles between fragments in addition to the fragmented CRC. Inserting synchronization sequences in front of every fragment provides complete decoupling among the fragments (proposed (I=1): I = 1, N=F, L=128 B×F^{-1}). Figure 7(b) shows that throughput is enhanced significantly to 60.1%. Despite of the effectiveness, a midamble occupies valuable channel bandwidth, and certainly it is a throughput limiting factor in high β conditions. Due to this fact, the fragmented CRC-only method performs better than proposed; (I=1) at α=1–5×10^{-3} and β=1–2×10^{-7} as shown in Fig. 7(b). To the contrary, by adjusting intervals of inserting midambles to each eight fragments (proposed (I=8): I=8, N=F/8, L=128 B×F^{-1}), the throughput is enhanced closely to the fragmented CRC of the condition of β=1. It is because the fragment error rate can be sufficiently suppressed with less number of midambles in this case. Hence, it is important to minimize the overhead of inserting midambles so that the benefit of midamble is not counterbalanced.

Table 1 shows the optimal L, I, and N parameters for each

3) A single packet is able to contain payload data up to 128 bytes in reliable communication mode (that is, R_{max} = 1). Throughput is normalized to the ideal throughput which is defined as the theoretical throughput bound, 5 Mbps, in absence of error corruptions and protocol overheads, such as preambles, error-detecting codes, and commands from a reader.

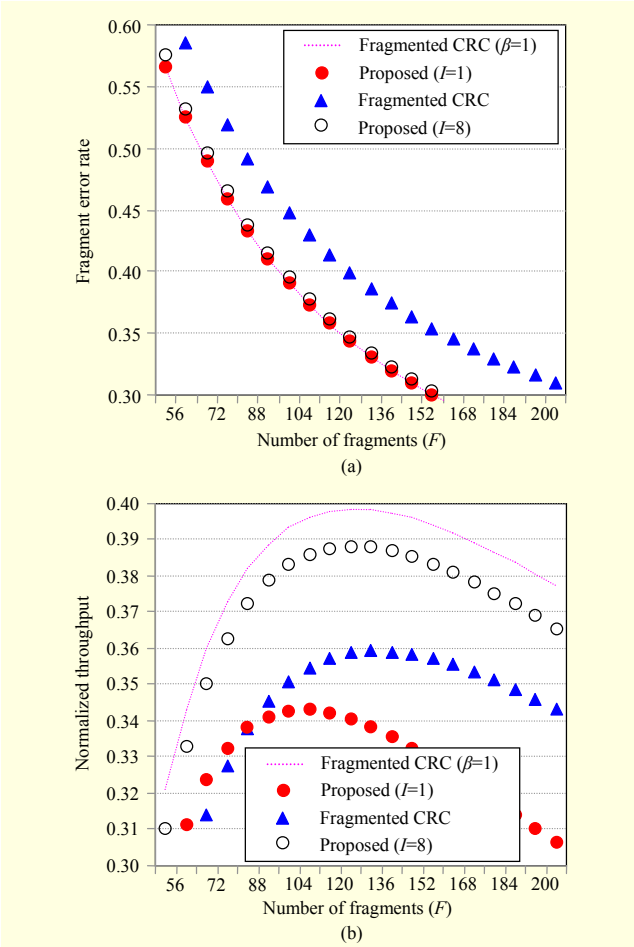

Fig. 7. Fragment error and throughput of each framing scheme at α =1–5×10^{-3}, β=1, and 1–2×10^{-7}.

packet framing scheme and the corresponding expected throughputs in reliable communication mode (R_{max}=∞) where the maximum amount of payload data in a single packet is limited to 1 kB. In this table, our proposed scheme is divided into two classifications: proposed-ideal and proposed-practical. For the proposed-ideal (also for packet CRC and fragment CRC), the parameter values were applied among all the possible natural numbers (in the case of L, the byte unit is used). In the case of the proposed-practical, parameter values were chosen in a set, $\{2^i: i$ is an integer, and $0 \le i \le 7\}$ (also, the unit of L is byte) to evaluate our proposed scheme with practically restricted parameter values.

For the packet CRC, fragment CRC, and proposed-ideal, it is clearly seen that there are prominent throughput improvements with the proposed scheme: up to 2.62 times of packet CRC and fragment CRC. As we evaluated with several link model parameters (α and β), fragmented CRC is not effective in poor link frequency conditions, that is low β. This is also shown in Table 1. At link conditions of v=1.25% and 2.50%, parameter I of fragmented CRC is just 1 in most case: it means that

Table 1. Optimal L/I/N parameters and expected throughput (TP, Mbps) ranges.

SNR	Packet CRC		Frag. CRC		Proposed-ideal		Proposed-practical	
	L	TP	L/I	TP	L/I/N	TP	L/I/N	TP
v = 0%, f = 0 Hz								
4	5	0.29	3/4	0.31	4/1/211	0.73	4/1/128	0.73
5	10	0.61	5/5	0.73	6/2/85	1.37	8/1/128	1.35
6	18	1.09	7/9	1.42	9/2/56	2.12	8/2/64	2.11
7	34	1.74	12/14	2.38	14/3/24	2.88	16/2/32	2.86
8	53	2.28	18/26	3.17	21/6/8	3.38	16/8/8	3.36
v = 0.50%, f = 10 kHz								
4	5	0.27	3/8	0.37	4/2/106	0.70	4/2/128	0.70
5	8	0.50	4/8	0.65	5/2/102	1.18	4/2/128	1.15
6	12	0.77	6/6	0.96	7/2/73	1.66	8/2/64	1.64
7	17	1.08	7/6	1.27	9/2/56	2.09	8/2/64	2.09
8	21	1.33	9/6	1.55	13/1/78	2.42	16/1/64	2.39
v = 1.25%, f = 10 kHz								
8	6	0.44	6/1	0.44	5/1/204	1.08	4/1/128	1.08
9	7	0.56	7/1	0.56	5/1/204	1.34	4/1/128	1.29
10	9	0.72	9/1	0.72	7/1/146	1.63	8/1/128	1.61
11	12	0.92	12/1	0.92	8/1/128	1.98	8/1/128	1.98
12	16	1.17	11/2	1.20	11/1/93	2.32	8/1/128	2.26
v = 2.50%, f = 10 kHz								
8	4	0.29	4/1	0.29	3/1/211	0.76	4/1/128	0.73
9	5	0.40	5/1	0.40	4/1/212	1.00	4/1/128	1.00
10	7	0.54	7/1	0.54	5/1/204	1.31	4/1/128	1.27
11	9	0.72	9/1	0.72	6/1/170	1.66	8/1/128	1.63
12	12	0.98	12/1	0.98	9/1/113	2.07	8/1/128	2.07

fragmentation cannot be applied for the optimal performance. However, the proposed scheme resolves this problem by employing more midambles at less accurate and stable link frequencies.

In the case of the proposed-practical, although the parameter value set is quite limited, the corresponding throughput degradations are quite negligible: 1.23% on average. Because a parameter value is a power of two, this restriction simplifies implementation. Therefore, it makes sense that the Streaming RFID protocol adopts this limited parameter value set and encodes each parameter in 3 bits: 9 bits in total.

2. Real-Time Video Streaming Over Streaming RFID

To evaluate effectiveness of the Streaming RFID protocol in

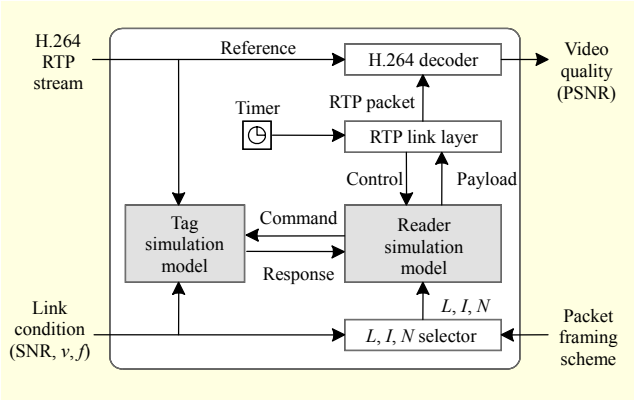

Fig. 8. Simulation environment for real-time H.264 video streaming.

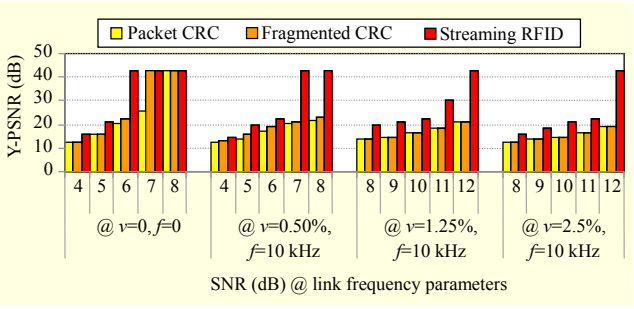

Fig. 9. Quality of received video in real-time H.264 streaming over the proposed Streaming RFID protocol.

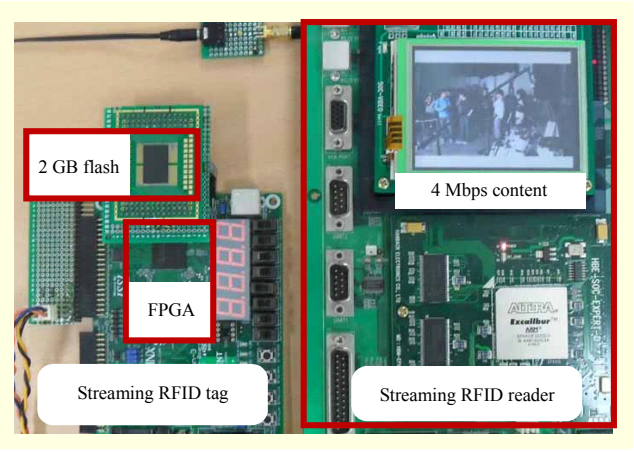

Fig. 10. Streaming RFID prototyped system.

real-time streaming applications, we experimented on real-time H.264 video streaming. The experiments used H.264 Real-Time Transport Protocol (RTP) streams which were generated by the H.264/AVC Joint Model Reference Software 16.2 [13]. The parameters for H.264 encoding are: 352×288 (CIF) foreman input sequence, 2 Mbps bitrate, 30 frames per second, 3,000 frames (duplicated 10 times from the original foreman), and fixed size (1,024 bytes) slice mode.

Figure 8 shows our experiment environment. As a simulation input, link conditions (SNR of AWGN channel, v and f of the link frequency model in (3)) were configured. For a given link condition, the optimal L, I, and N parameters of a packet framing scheme were selected according to Table 1 (Streaming RFID uses parameters of the proposed-practical in the table). The RTP link layer operates over the Streaming RFID reader. As the optimal payload length of Streaming RFID packets may differ from the length of original RTP packets, RTP link layer reconstructs RTP packets by splitting and assembling payloads received from the Streaming RFID reader.

A strategy of the link layer to support real-time streaming service follows. It monitors the reception status of RTP packets and estimates the arrival time of RTP packets which correspond to the video frame to be decoded next. If the arrival time is beyond the deadline of the frame, the link layer controls the reader to stops the retransmissions of error corrupted fragments and to skip several RTP packets until the deadline can be met. In other words, the reader does not request the transmission of RTP packets which cannot meet the deadline.

Figure 9 shows the experiment results for several link conditions. It is observed that Streaming RFID achieves higher visual quality than the packet and fragmented CRC schemes. While it is consistent with the results in Table 1, one might be concerned that a NACK command that is too long is unsuitable for real-time applications with time constraints. In the experiment, the Streaming RFID transfers a large number of fragments (I·N) in a single packet: up to 256 fragments, while up to 26 fragments in fragmented CRC scheme. A NACK command contains a retransmission mask, and the size of the mask is equal to the number of fragments. Therefore, overheads of sending a NACK command is non-trivial, especially in our system which has slow downlink speed: 5-times slower than the uplink. However, these experiment results show that the heavy overhead of NACK commands is not so serious because of low fragment error rates.

3. Impact on Hardware Implementation

To evaluate the impact of the Streaming RFID protocol on the hardware implementation, we made a prototype of the Streaming RFID tag by extending a traditional RFID tag as RFID-headphone did [3]. The implementation cost was a hardware complexity increment of 22% in the baseband modem with CMOS 0.18 μm technology. Also, the power consumption was estimated to be 19.6 μW, which is only 6.49 times higher although the prototyped tag supports 8 times faster data rate than the original tag. Including the rest of tag components, the total power consumption was estimated to be about 252 μW, which is sufficiently activated by a reader. We

verified the tag baseband modem using an FPGA, while RF/analog circuits were emulated by wired connection and pseudo noise injection between the tag and the corresponding reader. Figure 10 shows a demonstration of a media play service with the prototype system.

V. Conclusion

This paper proposed the Streaming RFID protocol in an effort to realize robust multimedia stream transmission over a passive RFID system.

In order to identify and resolve problems in realizing the system, a detailed analysis on packet framing schemes were presented by observing and modeling the bit error behavior at each bit location in a packet. It turned out that the size of a single packet is significantly limited by inaccurate and unstable link frequencies which are inevitable in the field of passive communications. It cannot be sufficiently resolved by only using the fragmented CRC. It is crucial to alleviate the problem of poor synchronization performance. As a promising solution, we proposed adaptive midamble embedding to provide re-synchronization points to a receiver. The midamble is adaptively combined with the fragmented CRC according to link conditions: accuracy and stability of a link frequency and SNR. This proposed method ensures rapid and robust transmission of massive multimedia streams over RFID at poor link conditions. Our proposal was evaluated by the H.264 video stream system, and prototyped in hardware only with a 22% hardware complexity increment from a traditional identification-purpose tag baseband modem.

The following are possible further studies for the academic and industry communities. First, we can develop and use accurate link frequency variation models to exactly capture the impact of the variation. Although a transistor level simulation model is available [12], it does not take into account the instability of power supply. Also, other research would be facilitated by developing a simple and accurate model at a higher level than that of a transistor. Second, we suggest examining other midamble insertion styles in an effort to reduce the fragmentation overhead. Our fragment basis midamble insertion to simplify implementation may be far from an optimal solution in some link conditions since the number of fragments must be equal to or larger than the number of midambles. This overhead might be alleviated by more flexible midamble insertion methods, for example, by allowing inserting multiple midambles in a fragment. Assume that synchronization losses are the only problem, and the bit decoding is quite accurate. In such cases, fragmented CRCs in front of every midamble just waste channel bandwidth without improving the performance. Third, fast and efficient packet framing parameter adaptation deserves further research. Relying on fragment error statistics, our packet framing parameter adaptation needs to collect a sufficiently large number of fragment error samples. Effectiveness of this method is limited to slowly varying link conditions. In RFID system, anti-collision is a popular hot research issue [14]-[16]. In a multiuser environment with our system, reader collision needs be more focused on than tag collision since tag collision only happens in an identification phase before actual streaming service.

The use model of the current available solution [4], which adopted the passive RFID technology in transferring large amounts of rich content, is limited by the touch-based interaction range communications. It is expected that the industry will pursue increasing the communication distance in order to provide more flexible and convenient connectivity from a tag to users. We believe that our work can satisfy the industry requirement by realizing robust streaming transmission over longer communication distances. However, long communication distances are vulnerable to data sniffing and security attacks; a malicious reader located within the communication range can capture all of the communication traffic, and masquerade as a tag by transmitting falsifying response packets. Large amounts of rich content stored in a tag can be commercial products or important confidential data. Therefore, the industry would have to pay more attention to security issues, although security in RFID has already been researched [17].

References

[1] ISO, "Information Technology–Radio Frequency Identification for Item Management–Part 6C: Parameters for Air Interface Communications at 860 MHz to 960 MHz," ISO/IEC 18000-6C Standard Document, International Organization for Standardization.

[2] R. Want, "Enabling Ubiquitous Sensing with RFID," *Computer*, vol. 37, no. 4, Apr. 2004, pp. 84-86.

[3] J.G. Lee et al., "Applying Passive RFID System to Wireless Headphones for Extreme Low Power Consumption," *Proc. 45th Annual Design Autom.Conf.*, 2008, pp. 486-491.

[4] J. McDonnell et al., "Memory Spot: A Labeling Technology," *IEEE Pervasive Computing*, vol. 9, no. 2, Apr.-June 2010, pp. 11-17.

[5] ISO, "Information Technology–Telecommunications and Information Exchange between Systems–Near Field Communication Interface and Protocol," ISO/IEC 21481, International Organization for Standardization.

[6] C. Wang et al., "Performance Analysis of RFID Generation-2 Protocol," *IEEE Trans. Wireless Commun.*, vol. 8, no. 5, May

2009, pp. 2592-2601.
[7] R.K. Ganti et al., "Datalink Streaming in Wireless Sensor Networks," *Proc. Int. Conf. Embedded Networked Sensor Syst.*, 2006, pp. 209-222.
[8] M. Chiani, A. Conti, and C. Fontana, "Improved Performance in TD-CDMA Mobile Radio System by Optimizing Energy Partition in Channel Estimation," *IEEE Trans. Commun.*, vol. 51, no. 3, Mar. 2003, pp. 352-355.
[9] S.D. Roemerman, "Radio Frequency Identification Interrogation Systems and Methods of Operating the Same," US Patent Pub., No. 20 07/0 035 383A1, 2007.
[10] Y. Liu et al., "Digital Correlation Demodulator Design for RFID Reader Receiver," *Proc. IEEE Wireless Commun. Networking Conf.*, Mar., 2007, pp. 1664-1668.
[11] S.J. Hwang et al., "A Low-Power Baseband Modem Architecture for a Mobile RFID Reader," *J. Embedded Computing*, vol. 3, no. 2, May 2009, pp. 131-140.
[12] F. Cilek et al., "Impact of the Local Oscillator on Baseband Processing in RFID Transponder," *Proc. Int. Symp. Signals, Syst., Electron.*, 2007, pp. 231-234.
[13] "JVT H.264/AVC Reference Software," Fraunhofer Heinrich Hertz Institute.
[14] X. Fan et al., "Gen2-Based Tag Anti-collision Algorithms Using Chebyshev's Inequality and Adjustable Frame Size," *ETRI J.*, vol. 30, no. 5, Oct. 2008, pp. 653-662.
[15] S.Y. Oh et al., "A Scheme to Increase Throughput in Framed-ALOHA-Based RFID Systems with Capture," *ETRI J.*, vol. 30, no. 3, June 2008, pp. 486-488.
[16] A. Mohsenian-Rad et al., "Distributed Channel Selection and Randomized Interrogation Algorithms for Large-Scale and Dense RFID Systems," *IEEE Trans. Wireless Commun.*, vol. 9, no. 4, Apr. 2010, pp. 1402-1413.
[17] P. Kitsos and Y. Zhang, *RFID Security: Techniques, Protocols and System-on-Chip Design*, New York: Springer, 2008.

Seok Joong Hwang received his BS and PhD from the School of Electrical Engineering of Korea University, Seoul, Rep. of Korea, in 2005 and 2011, respectively. Currently, he is a post doctoral researcher at the same department. His research interests include low-power SoC design, compiler construction, and high performance microprocessor architecture.

Youngsun Han received the BS and PhD from the School of Electrical Engineering of Korea University, Seoul, Rep. of Korea, in 2003 and 2009, respectively. He was a senior engineer at the System LSI division of Samsung Electronics, Rep. of Korea, from 2009 to 2011. He joined the School of Electrical Engineering at Kyungil University, Rep. of Korea, in 2011, where he is currently a full-time lecturer. His research interests include compiler design and optimization, SoC architecture, and design methodology.

Seon Wook Kim received the BS from the School of Electronics and Computer Engineering, Korea University, Seoul, Rep. of Korea, in 1988. He received the MS from the Department of Electrical Engineering, Ohio State University, Columbus, Ohio, USA, in 1990, and the PhD from the Department of Electrical and Computer Engineering, Purdue University, West Lafayette, Indiana, USA, in 2001. He was a senior researcher at the Agency for Defense Development from 1990 to 1995, and a staff software engineer at Intel/KSL from 2001 to 2002. Currently, he is a professor with the School of Electrical Engineering of Korea University. His research interests include compiler construction, microarchitecture, and SoC design. He is a senior member of ACM and a member of IEEE.

Jong-Ok Kim received the BS and MS in electronic engineering from Korea University, Seoul, Rep. of Korea, in 1994 and 2000, respectively, and the PhD in information networking from Osaka University, Osaka, Japan, in 2006. From 1995 to 1998, he served as an officer in the Korean Air Force. From 2000 to 2003, he was with SK Telecom R&D Center and Mcubeworks Inc., Rep. of Korea where he was involved in research and development on mobile multimedia systems. From 2006 to 2009, he was a researcher at the Advanced Telecommunication Research Institute International (ATR), Kyoto, Japan. He joined Korea University in 2009, where is currently an assistant professor. His current research interests are in the areas of multimedia communications, video compression, and wireless network QoS. Prof. Kim was a recipient of a Japanese Government Scholarship during 2003 to 2006.